ISM1 protects lung homeostasis via cell-surface GRP78-mediated alveolar macrophage apoptosis

Terence Y. W. Lam[a], Ngan Nguyen[a], Hong Yong Peh[b,c], Mahalakshmi Shanmugasundaram[a], Ritu Chandna[a], Jong Huat Tee[a], Chee Bing Ong[d], Md. Zakir Hossain[e], Shruthi Venugopal[a], Tianyi Zhang[a], Simin Xu[a], Tao Qiu[a], Wan Ting Kong[f], Svetoslav Chakarov[f], Supriya Srivastava[g], Wupeng Liao[b], Jin-Soo Kim[h,i], Ming Teh[j], Florent Ginhoux[f], W. S. Fred Wong[b,k,l], and Ruowen Ge[a,1]

[a]Department of Biological Sciences, Faculty of Science, National University of Singapore, Singapore 117543, Singapore; [b]Department of Pharmacology, Yong Loo Lin School of Medicine, National University of Singapore, Singapore 117600, Singapore; [c]Division of Pulmonary and Critical Care Medicine, Department of Internal Medicine, Brigham and Women's Hospital, Harvard Medical School, Boston, MA 02115; [d]Institute of Molecular and Cell Biology, Agency for Science, Technology, and Research, Singapore 138673, Singapore; [e]Cancer Science Institute of Singapore, National University of Singapore, Singapore 117599, Singapore; [f]Singapore Immunology Network, Agency for Science, Technology, and Research, Singapore 138648, Singapore; [g]Department of Medicine, National University Hospital, Singapore 119228, Singapore; [h]Center for Genome Engineering, Institute for Basic Science, Seoul 08826, South Korea; [i]Department of Chemistry, Seoul National University, Seoul 08826, South Korea; [j]Department of Pathology, National University Hospital, Singapore 119228; [k]Immunology Program, Life Science Institute, National University of Singapore, Singapore 117456, Singapore; and [l]Singapore–Hebrew University of Jerusalem Alliance for Research and Enterprise, National University of Singapore, Singapore 138602, Singapore

Edited by Augustine Choi, Cornell University, Ithaca, NY; received September 11, 2020; accepted November 20, 2021 by Editorial Board Member Carl F. Nathan

Alveolar macrophages (AMs) are critical for lung immune defense and homeostasis. They are orchestrators of chronic obstructive pulmonary disease (COPD), with their number significantly increased and functions altered in COPD. However, it is unclear how AM number and function are controlled in a healthy lung and if changes in AMs without environmental assault are sufficient to trigger lung inflammation and COPD. We report here that absence of isthmin 1 (ISM1) in mice (*Ism1*$^{-/-}$) leads to increase in both AM number and functional heterogeneity, with enduring lung inflammation, progressive emphysema, and significant lung function decline, phenotypes similar to human COPD. We reveal that ISM1 is a lung resident anti-inflammatory protein that selectively triggers the apoptosis of AMs that harbor high levels of its receptor cell-surface GRP78 (csGRP78). csGRP78 is present at a heterogeneous level in the AMs of a healthy lung, but csGRP78^{high} AMs are expanded in *Ism1*$^{-/-}$ mice, cigarette smoke (CS)-induced COPD mice, and human COPD lung, making these cells the prime targets of ISM1-mediated apoptosis. We show that csGRP78^{high} AMs mostly express MMP-12, hence proinflammatory. Intratracheal delivery of recombinant ISM1 (rISM1) depleted csGRP78^{high} AMs in both *Ism1*$^{-/-}$ and CS-induced COPD mice, blocked emphysema development, and preserved lung function. Consistently, ISM1 expression in human lungs positively correlates with AM apoptosis, suggesting similar function of ISM1–csGRP78 in human lungs. Our findings reveal that AM apoptosis regulation is an important physiological mechanism for maintaining lung homeostasis and demonstrate the potential of pulmonary-delivered rISM1 to target csGRP78 as a therapeutic strategy for COPD.

ISM1 | alveolar macrophages | apoptosis | cell surface GRP78 | chronic obstructive pulmonary disease

Chronic obstructive pulmonary disease (COPD) currently stands as the third leading cause of death globally with an estimated cumulated lifetime risk of 25% and high socioeconomical burden (1, 2). The pathogenesis of COPD involves perturbation of lung homeostasis and a dysregulated immune response to exogenous agents from the environment with cigarette smoke (CS), biomass fuel exposure, and air pollution as the main risk factors (3). Hallmark features of COPD include emphysema (the destruction of alveolar walls and enlargement of the alveoli) and chronic obstructive bronchitis (inflamed small airways). COPD patients present persistent respiratory symptoms with progressive long-term lung function decline. However, current drugs only provide symptomatic relief and are not able to suppress the underlying tissue inflammation to effectively block COPD progression or reduce mortality. Therefore, there is an urgent unmet need for novel COPD therapeutics targeting COPD pathophysiology (4).

Chronic lung inflammation is integral to COPD pathogenesis, and disease severity in COPD patients is directly associated with alveolar macrophage (AM) accumulation (5). These observations are concurred by mouse studies that exhibited complete protection against experimental COPD upon AM depletion (6) or knockout of the AM elastase MMP-12 (7). AMs are the first line of defense critical for lung homeostasis, pathogen recognition, debris clearance, resolution of lung inflammation, and repair of damaged tissue. AMs are phenotypically and functionally highly plastic in response to their environment. Under physiological conditions, AMs contribute to the prevention of inflammatory response from occurring and

Significance

Inflammation regulation and homeostasis maintenance is of paramount importance for lung health. Using both genetic and pathological mouse models, this work reveals that the secreted proapoptotic isthmin 1 (ISM1) protects lung homeostasis by controlling alveolar macrophage (AM) population and functional phenotype via cell-surface GRP78 (csGRP78)-mediated apoptosis. In both mouse and human, AMs express varied amount of csGRP78, enabling ISM1 to selectively remove the proinflammatory csGRP78^{high} AMs via apoptosis. In cigarette smoke–induced chronic obstructive pulmonary disease (COPD) mice, pulmonary delivery of recombinant ISM1 (rISM1) suppressed lung inflammation, blocked emphysema development, and preserved lung function. This work reveals molecular insights for lung homeostasis regulation and offers a rationale to target csGRP78 with pulmonary-delivered rISM1 as a potential therapeutic strategy for COPD.

Author contributions: R.G. designed research; T.Y.W.L., N.N., H.Y.P., M.S., R.C., J.H.T., M.Z.H., S.V., T.Z., S.X., T.Q., W.T.K., S.C., S.S., W.L., and J.-S.K. performed research; T.Y.W.L., C.B.O., M.T., F.G., W.S.F.W., and R.G. analyzed data; and T.Y.W.L. and R.G. wrote the paper.

Competing interest statement: R.G. is the scientific founder of NovoBreeze Therapeutics Co. Ltd, a private biopharma company.

This article is a PNAS Direct Submission. A.C. is a guest editor invited by the Editorial Board.

[1]To whom correspondence may be addressed. Email: dbsgerw@nus.edu.sg.

This article contains supporting information online at http://www.pnas.org/lookup/suppl/doi:10.1073/pnas.2019161119/-/DCSupplemental.

Published January 19, 2022.

produce immunosuppressive factors (8–10). The number of AMs in a healthy mouse lung is maintained at around 0.3 to 1 per alveolus, while AM numbers in human lungs are around 4 to 5 per alveolus (9, 11–13). AM numbers and functional phenotypes are altered with age in nonsmokers, active smokers, and patients with COPD, with AMs as the key effector cells for COPD (5, 14–17). However, it is not clear how AM numbers and functions are controlled in a healthy lung and whether an increase in AM number or change in AM function without any environmental assault (such as CS) would be sufficient to cause lung pathologies.

We have previously identified isthmin 1 (ISM1) as a secreted proapoptotic protein that functions through cell-surface GRP78 (csGRP78, high-affinity receptor) and αvβ5 integrin (low-affinity receptor) via two distinct apoptotic pathways (18, 19). Specifically, recombinant ISM1 (rISM1) binds to αvβ5 integrin and activates caspase-8 or binds to csGRP78, where it is endocytosed and trafficked to mitochondria, inhibiting ATP production and triggering apoptosis by inducing mitochondria dysfunction. Nevertheless, the physiological function of *Ism1* remains to be fully elucidated.

In this work, we report that ISM1 plays a critical role in maintaining mouse lung homeostasis by controlling AM numbers through csGRP78-mediated apoptosis. The knockout of *Ism1* in mice (*Ism1*$^{-/-}$ mice) leads to an increase in csGRP78^{high} AM numbers with accompanied MMP-12 up-regulation, chronic lung inflammation, and progressive emphysema. We further show that pulmonary delivery of rISM1 effectively quenched lung inflammation by depleting the proinflammatory csGRP78^{high} AMs via targeted apoptosis, blocking emphysema progression and preserving lung function in CS-induced COPD mice. Correspondingly, ISM1 expression in the human lung correlates with increased AM apoptosis, with csGRP78 highly up-regulated in the AMs of COPD patients. Our work reveals an anti-inflammatory role of ISM1 in maintaining lung homeostasis and underscores the potential of targeted AMs apoptosis via ISM1–csGRP78 as a therapeutic strategy for COPD.

Results

***Ism1*$^{-/-}$ Mice Develop Spontaneous Emphysema.** *Ism1* expression is highest in both fetal and adult mouse lungs, almost 30-fold higher than its second highest expressing organ, the brain (20–22). To study its physiological function, we generated *Ism1* knockout (*Ism1*$^{-/-}$) mice using the CRISPR/Cas9 approach in two different strains of mice: FVB/NTac and C57BL/6J (*SI Appendix*, Fig. S1 *A–D*). *Ism1*$^{-/-}$ mice are viable, reproductively competent, and present no gross behavioral phenotype. A histopathology examination of major organs revealed that *Ism1*$^{-/-}$ mice developed spontaneous and progressive emphysema in both mouse strains (Fig. 1 *A* and *B* and *SI Appendix*, Fig. S1 *E–G*). These results support a role of ISM1 in lung homeostasis, consistent with its highest expression in lungs. As the emphysema phenotype is more pronounced in the FVB/NTac strain, we subsequently mainly used FVB/Ntac *Ism1*$^{-/-}$ mice for this study. Fluorescent labeling of collagen and elastin showed deterioration of the alveolar extracellular matrix network in *Ism1*$^{-/-}$ lungs (Fig. 1*C*). A Verhoeff–Van Gieson stain revealed loss of elastin fibers and ruptured septa in *Ism1*$^{-/-}$ lungs (*SI Appendix*, Fig. S1*H*). In addition, heterozygous *Ism1*$^{+/-}$ mouse lung expresses intermediate amounts of ISM1 between those of wild-type (WT) and *Ism1*$^{-/-}$ lungs accompanied with milder emphysema (Fig. 1 *D–G*), suggesting that *Ism1* is haploinsufficient for lung homeostasis in mice.

Pulmonary function tests on 2-mo-old *Ism1*$^{-/-}$ mice showed increased total lung capacities (Fig. 1*H*) and volume compartments (Fig. 1 *I* and *J*) synonymous with hyper-inflated lungs observed in COPD patients because of loss of elastic recoil and air trapping associated with emphysema (23). These changes were also reflected in pressure–volume measurements whereby both static and dynamic compliance were increased in *Ism1*$^{-/-}$ mice (Fig. 1 *K* and *L*). Importantly, *Ism1*$^{-/-}$ mice displayed lower forced expiratory volumes (Fig. 1*M*) and possessed means of forced expiratory volume at 100 ms/forced vital capacity (FEV_{100}/FVC, equivalent to the FEV_1/FVC index in human COPD) of <0.7 (Fig. 1*N*, *Ism1*$^{-/-}$: 0.63 ± 0.05), a criterion routinely used for COPD diagnosis in patients (3). Increased airway resistance in *Ism1*$^{-/-}$ mice may be attributed to mucus hypersecretion and inflammatory changes in the airway wall (Fig. 1*O* and *SI Appendix*, Fig. S1 *I* and *J*) (24). Collectively, these data showed that *Ism1*$^{-/-}$ mice presented similar lung pathologies to experimental mouse COPD models and human COPD patients.

No gross histological abnormalities were observed in other major organs of *Ism1*$^{-/-}$ mice at 2 mo of age, including the brain (*SI Appendix*, Fig. S2*A*). Immunofluorescence (IF) staining of cleaved caspase-3 showed minimum apoptosis in the brain of both WT and *Ism1*$^{-/-}$ mice at this age (*SI Appendix*, Fig. S2*B*). In this work, we focused on ISM1's function in the lung.

AMs Drive Emphysema in *Ism1*$^{-/-}$ Lungs. Emphysema in *Ism1*$^{-/-}$ mice is accompanied by increased and multifocal aggregates of AMs as confirmed by lung histology as well as cytospin and flow cytometric analysis of cells from bronchoalveolar lavage fluid (BALF) (Fig. 2 *A–D*). Notably, AMs from *Ism1*$^{-/-}$ lungs comprise residential AMs ($CD45^+Siglec\text{-}F^+CD11c^+$) with no obvious infiltration of monocyte-derived AMs ($CD45^+CD11b^+Ly6C^{+/-}$) (*SI Appendix*, Fig. S3). *Ism1*$^{-/-}$ AMs display more heterogeneous morphologies including size variation and the presence of some giant multinucleated cells, similar to macrophage subpopulations under lung inflammation and in COPD patients (25) (Fig. 2 *A* and *B* and *SI Appendix*, Fig. S4 *A* and *B*). Nevertheless, isolated primary AMs from *Ism1*$^{-/-}$ mouse lungs presented similar efferocytosis capacity in vitro as those of the WT mice (*SI Appendix*, Fig. S4*C*).

Western blot analysis of *Ism1*$^{-/-}$ lung lysates revealed increased levels of MMP-12, MMP-9, and NF-κB p65 (Fig. 2*E*) as well as increased MMP-9 and MMP-2 activity by gelatin zymography (*SI Appendix*, Fig. S4*D*). Immunohistochemistry (IHC) staining identified that AMs express and contribute to the increased MMP-12 and MMP-9 in *Ism1*$^{-/-}$ lungs (Fig. 2*F*), consistent with COPD pathology (26). Moreover, isolated primary AMs from *Ism1*$^{-/-}$ mice showed increased nuclear translocation of NF-κB p65, indicating NF-κB activation (Fig. 2*G*). In addition, TGF-β1 and VEGF-A were moderately up-regulated in *Ism1*$^{-/-}$ lungs (*SI Appendix*, Fig. S4 *E* and *F*) in line with observations in COPD patients along with higher levels of reactive oxygen species (*SI Appendix*, Fig. S4*G*) (27, 28). In contrast, neither neutrophil elastase nor alpha-1-antitrypsin levels showed any differences between *Ism1*$^{-/-}$ and WT mice (*SI Appendix*, Fig. S4*E*). A multiplex enzyme-linked immunosorbent assay array analysis of *Ism1*$^{-/-}$ lungs showed up-regulated inflammatory cytokines including IL-1α, G-CSF, GM-CSF, MIP-1α, and MCP-2 (*SI Appendix*, Fig. S4*H*). Since GM-CSF drives AM development (29) and GM-CSF–overexpressing mice develop emphysema with AM accumulation (30), we analyzed GM-CSF in *Ism1*$^{-/-}$ mouse lungs. Western blots of postnatal mouse lungs showed no difference in GM-CSF levels between *Ism1*$^{-/-}$ and WT mice at P1, P7, and 1 mo of age (*SI Appendix*, Fig. S4*I*). However, MMP-12 is progressively up-regulated from P7 *Ism1*$^{-/-}$ lungs (*SI Appendix*, Fig. S4*I*). By 2 mo of age, both MMP-12 and GM-CSF are higher in *Ism1*$^{-/-}$ mouse lungs (Fig. 2 *E* and *H*). Thus, MMP-12 up-regulation precedes that of GM-CSF, suggesting that GM-CSF was likely up-regulated as the result of lung inflammation and emphysema in 2-mo-old *Ism1*$^{-/-}$ lungs.

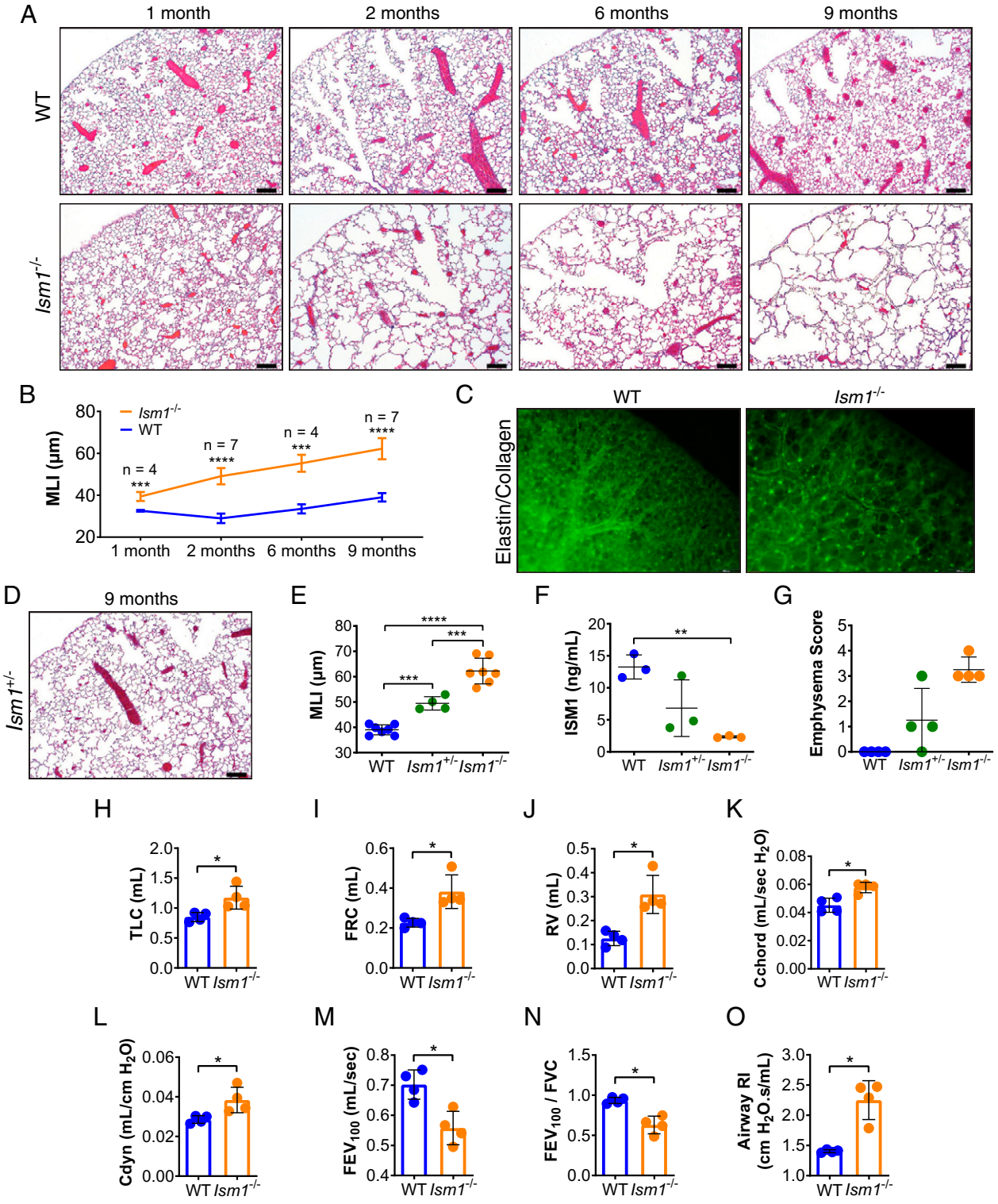

Fig. 1. Loss of ISM1 leads to pulmonary emphysema in mice. (*A*) Hematoxylin and eosin (H&E) stained left lungs and (*B*) mean linear intercepts (MLI) of FVB/NTac WT and *Ism1*$^{-/-}$ mice at 1, 2, 6, and 9 mo of age. (*C*) Whole-mount stereoscopic elastin/collagen-labeled left lungs of FVB/NTac WT and *Ism1*$^{-/-}$ mice at 6 mo of age. (*D*) H&E stained left lung of FVB/NTac *Ism1*$^{+/-}$ mice at 9 mo of age. (*E*) MLI of FVB/NTac WT, *Ism1*$^{+/-}$, and *Ism1*$^{-/-}$ mice at 9 mo of age. (*F*) ISM1 protein level in FVB/NTac WT, *Ism1*$^{+/-}$, and *Ism1*$^{-/-}$ lungs at 2 mo of age determined by enzyme-linked immunosorbent assay. (*G*) Pathology grading of emphysema in FVB/NTac WT, *Ism1*$^{+/-}$, and *Ism1*$^{-/-}$ mice at 2 mo of age. (*H–O*) Spirometry of FVB/NTac WT and *Ism1*$^{-/-}$ mice at 2 mo of age. (*H*) Total lung capacity, (*I*) functional residual capacity, (*J*) residual volume, (*K*) static compliance, (*L*) dynamic compliance, (*M*) forced expiratory volume at 100 ms (FEV_{100}), (*N*) Tiffeneau–Pinelli index (FEV_{100}/FVC), and (*O*) airway resistance. Data are mean ± SD and were analyzed by two-group, two-tailed Student's *t* test (*B* and *H–O*), and one-way ANOVA with Tukey's post hoc test (*E* and *F*). **P* < 0.05, ***P* < 0.01, ****P* < 0.001, and *****P* < 0.0001. *n* = 3 to 7 mice per group. (Scale bars, 200 μm for *A*, *C*, and *D*.) Data from *A* and *B* are integrated from two independent experiments (biological repeats, *n* = 7) except for MLI data for 1- and 6-mo-old mouse groups, which are from one independent experiment (*n* = 4). Data from *C–G* are independent experiments using different WT and *Ism1*$^{-/-}$ mice. Data from *H–O* are independent experiments using the same WT and *Ism1*$^{-/-}$ mice.

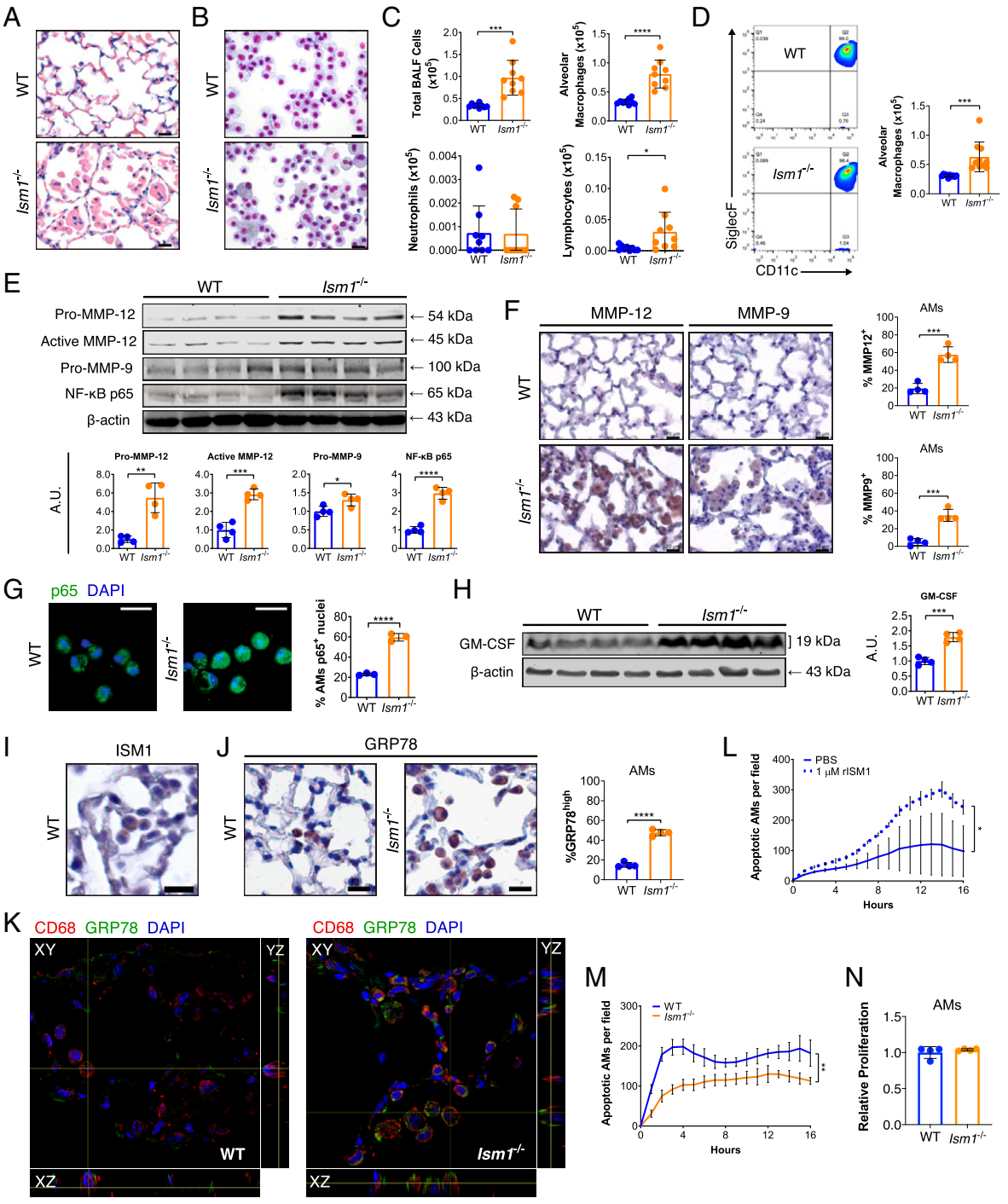

Fig. 2. *Ism1*$^{-/-}$ mouse lungs present up-regulated COPD mediators at 2 mo of age. (*A*) H&E stained lungs showing focal AM accumulation in FVB/NTac *Ism1*$^{-/-}$ mice. (*B*) Liu-stained cytospins and (*C*) quantifications of BALF cells from FVB/NTac WT and *Ism1*$^{-/-}$ lungs. (*D*) Flow cytometric analysis and quantifications of AMs (Siglec F^{+} CD11c^{+}) in BALF from FVB/NTac WT and *Ism1*$^{-/-}$ lungs. (*E*) Western blots and quantification of fold changes for Pro-MMP-12, Active-MMP-12, Pro-MMP-9, and NF-κB p65 with β-actin as loading control in FVB/NTac WT and *Ism1*$^{-/-}$ lungs. (*F*) IHC and quantifications of MMP-12^{+} and MMP-9^{+} AMs of FVB/NTac WT and *Ism1*$^{-/-}$ lungs. (*G*) IF staining for NF-κB p65 with nuclei counterstain (DAPI) and quantification of primary AMs harboring nuclear p65^{+} from FVB/NTac WT and *Ism1*$^{-/-}$ mice. (*H*) Western blot and fold change for GM–CSF with β-actin as loading control in FVB/NTac WT and *Ism1*$^{-/-}$ lungs. (*I*) IHC for ISM1, and (*J*) IHC for GRP78 and quantification of GRP78^{high} AMs in FVB/NTac WT and *Ism1*$^{-/-}$ mice. (*K*) Confocal fluorescent microscopy image demonstrating csGRP78^{high} AMs in FVB/NTac WT and *Ism1*$^{-/-}$ lungs. (*L*) rISM1 induces apoptosis in WT primary AMs. (*M*) Apoptosis of freshly isolated primary AMs from FVB/NTac WT and *Ism1*$^{-/-}$ lungs. Analysis was carried out in triplicate or quadruplicate wells. (*N*) Proliferation of primary AMs from WT and *Ism1*$^{-/-}$ mice. Analysis was carried out in triplicate wells. Data are mean ± SD and were analyzed by two-group, two-tailed Student's *t* test (*C–H*, *J*, and *L–N*). **P* < 0.05, ***P* < 0.01, ****P* < 0.001, and *****P* < 0.0001. *n* = 3 to 10 mice per group. A.U.: arbitrary units. (Scale bars, 20 μm for *A*, *B*, *F*, *G*, *I*, and *J*.) Data from *C* and *D* are integrated from two independent experiments using different WT and *Ism1*$^{-/-}$ mice (biological repeats, *n* = 9 to 10). Data from *E–M* are representatives of twice-repeated experiments with similar results. Data from *N* is from one independent experiment.

Although a mild reduction of radial alveolar count is detected in *Ism1*$^{-/-}$ mouse lungs at 1 mo of age, the impact of ISM1 deficiency on alveolar simplification is likely minor, as most emphysematous changes occur after alveolar maturation from 1 mo of age (*SI Appendix*, Fig. S5*A*) (31, 32), suggesting that progressive emphysema is likely a result of alveolar wall destruction. This is supported by the similar distribution of types 1 and 2 alveolar epithelial cells and proliferating parenchymal cells in the lungs of 1-mo-old *Ism1*$^{-/-}$ and WT mice (*SI Appendix*, Fig. S5 *B*–*E*). Neither vascular density nor integrity were altered in nonemphysematous areas of *Ism1*$^{-/-}$ mouse lungs as demonstrated by similar endothelial (endomucin) and tight junction (occludin) staining (*SI Appendix*, Fig. S5*F*) as well as normal levels of BALF protein content (*SI Appendix*, Fig. S5*G*).

ISM1 expression was previously reported in mouse bronchial and alveolar epithelium (20, 21). Here, we show that AMs are an additional source of ISM1 (Fig. 2*I* and *SI Appendix*, Fig. S6 *A* and *B*), although not all AMs constitutively express ISM1 in the healthy lung. Strikingly, AMs in *Ism1*$^{-/-}$ lungs present more distinct periplasmic GRP78 staining compared to WT mice (Fig. 2*J*), but no αvβ5 integrin expression is detected (*SI Appendix*, Fig. S6*C*). csGRP78 has been previously reported on mouse peritoneal macrophages (33) and human monocytes (34). To verify if csGRP78 serves as the ISM1 receptor on AMs, we first demonstrated that GRP78 is localized on AM cell surface by confocal fluorescent microscopy. In *Ism1*$^{-/-}$ lungs, higher levels of csGRP78 are present on more AMs (Fig. 2*K* and *SI Appendix*, Fig. S6*D*). We treated primary AMs with rISM1 and observed that rISM1 binds to csGRP78 of nonpermeabilized AMs (*SI Appendix*, Fig. S6*E*) and induces AM apoptosis (Fig. 2*L*). Similarly, rISM1 potently induced apoptosis in immortalized mouse AM cells (MH-S) pretreated with thapsigargin, an endoplasmic reticulum (ER) stress inducer known to promote GRP78 translocation to cell surface (35), and dose dependently increased csGRP78 expression in MH-S cells (*SI Appendix*, Fig. S6 *F* and *G*). Consistent with our previous studies on endothelial cells (19, 36), rISM1-induced apoptosis in MH-S cells is mediated by its translocation to mitochondria (*SI Appendix*, Fig. S6*H*). Moreover, anti-GRP78 antibody neutralization and small interfering RNA knockdown of GRP78 attenuated rISM1-induced apoptosis in MH-S cells (*SI Appendix*, Fig. S6 *I*–*K*), demonstrating that ISM1 induces apoptosis through csGRP78. Concomitantly, primary AMs isolated from *Ism1*$^{-/-}$ mice showed reduced apoptosis but no difference in proliferation (Fig. 2 *M* and *N* and *SI Appendix*, Fig. S6*L*). These results support the notion that the absence of endogenous ISM1–csGRP78-mediated autocrine/paracrine apoptosis may lead to csGRP78^{high} AM accumulation, which could be linked to MMP up-regulation and spontaneous emphysema in *Ism1*$^{-/-}$ lungs.

rISM1 Rescues Emphysema in *Ism1*$^{-/-}$ and CS-Induced COPD Mice. Since AMs are pivotal to COPD pathogenesis, we evaluated if pulmonary-delivered rISM1 could rescue *Ism1*$^{-/-}$ lung from emphysema by promoting csGRP78^{high} AM apoptosis. Intratracheal rISM1 was delivered twice weekly to 1-mo-old *Ism1*$^{-/-}$ mice for 4 wk and compared to treatments by vehicle or liposome-clodronate, an established agent for AM depletion. Immunostainings showed that rISM1 was internalized by AMs and induced apoptosis (*SI Appendix*, Fig. S7 *A* and *B*), reducing AM numbers in a dose-dependent manner (Fig. 3*A*). Importantly, rISM1 treatment reduced csGRP78^{high} AMs in *Ism1*$^{-/-}$ lung (Fig. 3*B*). More importantly, csGRP78^{high} AMs are also predominantly MMP-12^{+}, an indication that these AMs are proinflammatory (*SI Appendix*, Fig. S7*C*). Both rISM1 and clodronate-treated *Ism1*$^{-/-}$ mouse lungs exhibited significant reductions in emphysema (Fig. 3 *C* and *D*), likely facilitated by alveolar regeneration following inflammation resolution as demonstrated by increased proliferating type II pneumocytes in both treated groups (*SI Appendix*, Fig. S7 *D* and *E*). Furthermore, airflow was partially restored in both rISM1 and clodronate-treated *Ism1*$^{-/-}$ mice (Fig. 3*E*). These results confirm that excessive csGRP78^{high} AMs are central to spontaneous emphysema and lung function decline in *Ism1*$^{-/-}$ mice. Pulmonary delivery of rISM1 can rescue the *Ism1*$^{-/-}$ emphysema phenotype through csGRP78^{high} AM depletion.

We next assessed if rISM1 could alleviate CS-induced lung inflammation or COPD in mice since chronic AM inflammation is tied to lung tissue damage. WT BALB/c mice were exposed to 2 wk (acute) and 8 wk (chronic) of CS or room air (sham) and intratracheally treated with either rISM1 or vehicle (Fig. 3 *F* and *G*). The 8-wk chronic CS regimen adopted has been previously established to effectively and reproducibly generate mild emphysema with FEV_{100}/FVC reduced to around 0.8 (37). Cytospin analysis of BALF cells from 2-wk CS-exposed mice revealed that rISM1 effectively suppressed CS-induced acute inflammation and reduced total BALF cells, AMs, and neutrophils without affecting lymphocytes (Fig. 3*H*). Histological analyses of 8-wk CS-exposed mouse lungs showed emphysema proximal to the terminal bronchioles with AM accumulation, similar to COPD patients who smoke (Fig. 3*I* and *SI Appendix*, Fig. S7*F*). CS exposure lead to more csGRP78^{high} AMs accompanied by MMP-12 up-regulation (MMP-12^{+}) (Fig. 3*J* and *SI Appendix*, Fig. S7*G*). Accordingly, rISM1 treatment enhanced AM apoptosis with significant reduction in GRP78^{high} AMs (Fig. 3 *K* and *L* and *SI Appendix*, Fig. S7*H*). Furthermore, significant reductions in active MMP-12 levels (Fig. 3*M*) and the number of neutrophils were also observed (*SI Appendix*, Fig. S7*I*). Correspondingly, rISM1 effectively blocked emphysema development (Fig. 3*N*) and preserved lung function (Fig. 3*O* and *SI Appendix*, Fig. S7 *J*–*L*) in CS-induced COPD mice. Consistently, GRP78 expression is notably up-regulated in cultured mouse AM MH-S cells upon treatment with cigarette smoke extract (CSE), while the addition of rISM1 potently induced apoptosis of GRP78^{high} MH-S cells (*SI Appendix*, Fig. S7 *M* and *N*).

ISM1 Expression Correlates with AM Apoptosis. Since *Ism1*$^{-/-}$ mice developed spontaneous emphysema and exogenously supplied rISM1 protected mice from CS-induced emphysema by inducing csGRP78-mediated AM apoptosis, we envisaged that variations in endogenous ISM1 levels in the human lung may also influence the development of COPD. We first validated antibody specificity for human ISM1 (hISM1) and GRP78 in immunostaining using cultured cells and antigen preadsorption (*SI Appendix*, Fig. S8 *A* and *B*) and subsequently examined hISM1 and GRP78 expression in lung tissue sections from 60 COPD and 18 non-COPD patients (*SI Appendix*, Table S1). Similar to mice, hISM1 is also expressed in AMs (Fig. 4 *A* and *B*). However, while ISM1 is also expressed in mouse bronchial epithelium, particularly after CS exposure (*SI Appendix*, Fig. S8*C*), hISM1 was generally not detected in bronchial epithelium in either COPD or non-COPD human lungs (*SI Appendix*, Fig. S8*D*). When we graded hISM1 expression by scoring both IHC staining intensity and frequency of hISM1 expression in AMs, we found that AM apoptosis was significantly increased with higher hISM1 expression (Fig. 4*C*). Furthermore, multiple linear regression analyses revealed that hISM1 expression is significantly correlated with AM apoptosis after adjustment for age, sex, smoking status, Global Initiative for Chronic Obstructive Lung Disease (GOLD) scores, and GRP78 expression (*SI Appendix*, Table S2). Nevertheless, no significant trend between hISM1 expression and COPD status was observed (*SI Appendix*, Fig. S8*E* and Table S3, $P = 0.372$). High GRP78 expression in AMs significantly and positively correlated with AM apoptosis via Pearson's correlation (Fig. 4*D*), and multiple

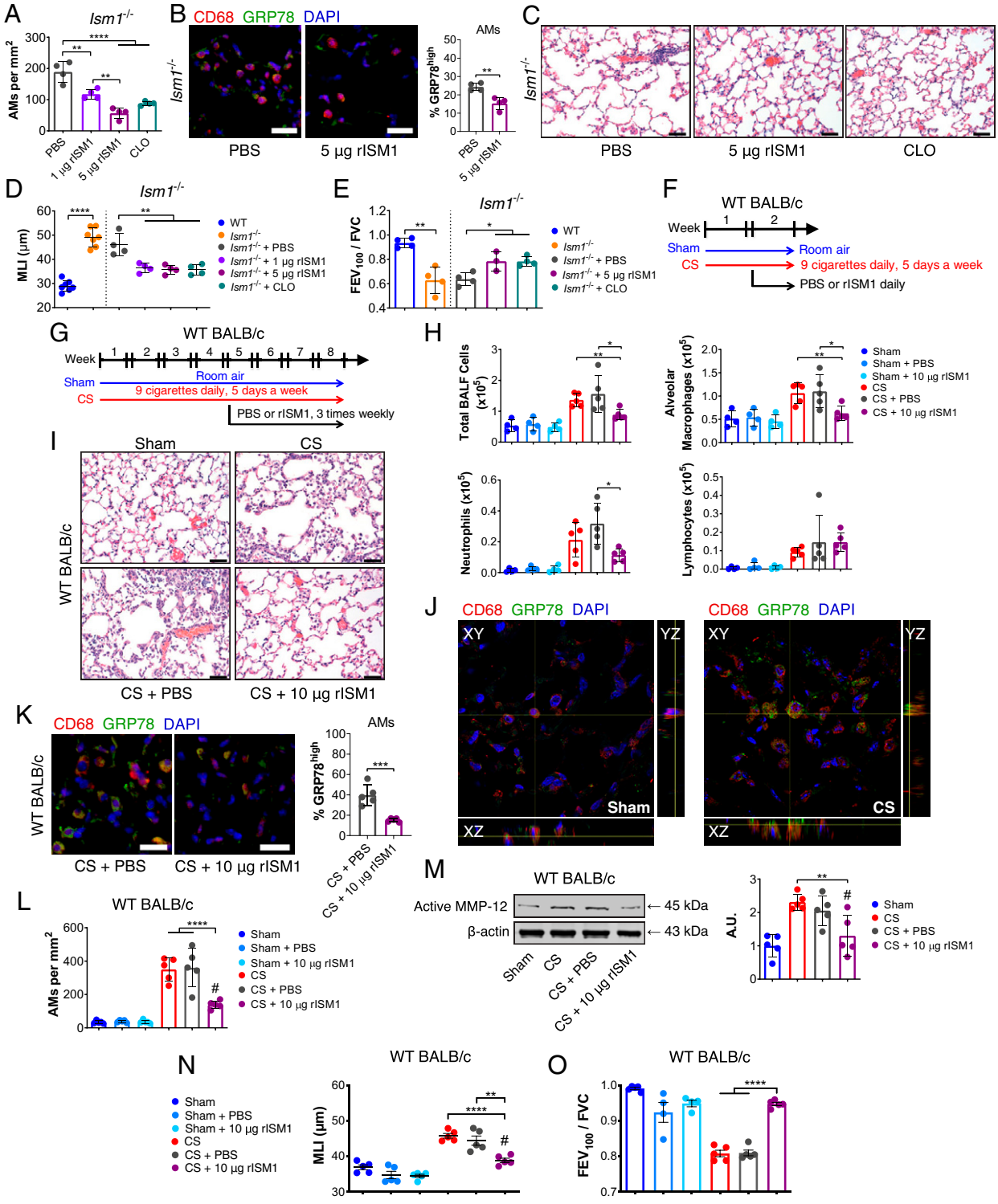

Fig. 3. Intratracheal-delivered rISM1 alleviates emphysema in *Ism1*$^{-/-}$ and CS-exposed mice. (*A*) Quantification of AMs from *Ism1*$^{-/-}$ lung under PBS, rISM1, and liposome-clodronate (CLO) treatments. (*B*) IF staining and quantifications for GRP78^{high}CD68^{+} AMs, nuclei are stained by DAPI. (*C*) Representative H&E-stained lungs of 2-mo-old FVB/NTac *Ism1*$^{-/-}$ mice after vehicle (PBS), 1 μg rISM1, 5 μg rISM1, and CLO treatments. (*D*) Quantifications of MLI and (*E*) FEV_{100}/FVC of untreated and treated mice groups in *A*. (*F*) Experimental design of 2-wk and (*G*) 8-wk CS-induced COPD model in WT BALB/cAnNTac (WT BALB/c) mice. Room air–exposed WT BALB/c mice (Sham) and CS-exposed WT BALB/c mice (CS) with vehicle (PBS) or rISM1 (10 μg rISM1) treatments at frequency and intervals indicated. (*H*) Quantifications of BALF cells from experimental groups in *F*. (*I*) H&E stained lungs of experimental groups in (*G*) depicting immune cell infiltration. $n = 5$ mice per group. (*J*) Confocal fluorescent microscopy demonstrating cell-surface expression of GRP78 in AMs in Sham and CS mouse lungs in *G*. (*K*) IF staining and quantifications of GRP78^{high} AMs and (*L*) total AMs for experiment groups in *G*. (*M*) Active MMP-12 detected by Western blot and their quantifications for experiment groups in *G*. (*N*) MLI and (*O*) FEV_{100}/FVC of experimental groups in *G*. Data are mean ± SD and were analyzed by two-group, two-tailed Student's *t* test (*B*, *D*, and *E:* WT and *Ism1*$^{-/-}$ comparisons; and *K*) and one-way ANOVA with Tukey's post hoc test (*A*, *D*, *E*, *H*, and *L*–*O*). *$P < 0.05$, **$P < 0.01$, ***$P < 0.001$, and ****$P < 0.0001$, #: no significant difference compared to Sham group. $n = 3$ to 5 mice per group. (Scale bars: 20 μm for *B* and *K*, 50 μm for *C* and *I*.) Data from *A*–*E* are representatives of twice-repeated experiments with similar results. Data from *H* is representative of one independent experiment. Data from *I*–*O* are independent experiments using the same experimental groups of mice in *L*.

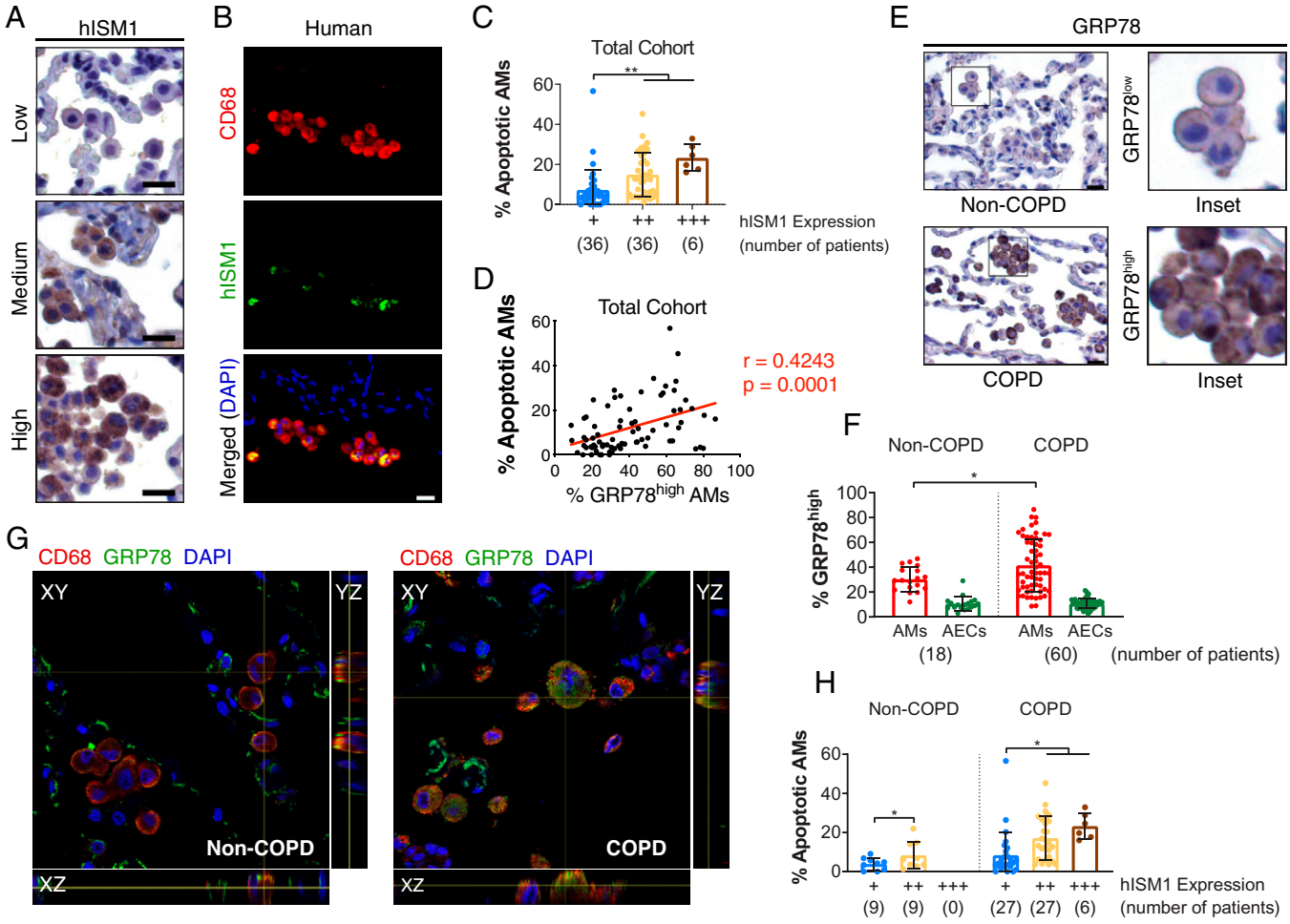

Fig. 4. hISM1 expression correlates with AM apoptosis. (*A*) IHC staining for hISM1 and (*B*) double IF staining for CD68 and hISM1 with nuclei (DAPI) counterstain in lung tissue sections showing AM expression of hISM1. (*C*) Quantifications of AM apoptosis in different hISM1 expression level groups. (*D*) Correlation analyses between high GRP78 expression with AM apoptosis. (*E*) Representative IHC for GRP78 depicting low GRP78 expression in non-COPD AMs and high GRP78 expression in COPD AMs. (*F*) Percentage of AMs and alveolar epithelial cells (AECs) in non-COPD and COPD patients with GRP78^{high} expression (*E*, COPD *Inset*). (*G*) Confocal microscopy images for CD68, GRP78, and nuclei (DAPI) in non-COPD and COPD human lungs. (*H*) Percentage of apoptotic AMs stratified by COPD status and hISM1 expression. Data are mean ± SD and were analyzed by Pearson correlation (*D*), one-way ANOVA (*C*), and two-way ANOVA (*F* and *H*) with Tukey's post hoc test. Patient sample sizes are depicted on graphs. (Scale bars, 20 μm for *A*, *B*, and *E*.)

linear regression analysis revealed GRP78 expression as another determinant of AM apoptosis after adjustments (*SI Appendix*, Table S2). Similar to CS-exposed mice, csGRP78^{high} AMs are predominantly present in the lungs of COPD patients (Fig. 4 *E*–*G*), suggesting that these AMs could be the prime targets for ISM1–csGRP78-mediated apoptosis. Consequently, more apoptotic AMs were observed in COPD patients with higher hISM1 expression (Fig. 4*H*), and most apoptotic cells were csGRP78^{high} AMs in both COPD patients and CS-exposed mouse lungs (*SI Appendix*, Fig. S8*F*). Meanwhile, hISM1 seems to be expressed in both csGRP78$^{low/-}$ and csGRP78^{high} AMs in human lungs (*SI Appendix*, Fig. S8*G*).

Consistently, csGRP78^{high} AMs were less apoptotic in C57BL/6J *Ism1*$^{-/-}$ mice compared to those of WT mice after 2 wk of CS exposure, further supporting the role of ISM1 in preventing csGRP78^{high} AM accumulation and the accompanied inflammation in *Ism1*$^{-/-}$ mice (*SI Appendix*, Fig. S8 *H* and *I*). These results support the notion that ISM1 selectively targets csGRP78^{high} AMs for apoptosis in both mouse and human lungs.

Expectedly, AMs are increased in smokers with COPD (*SI Appendix*, Fig. S9*A*), and there is a statistically significant trend between higher hISM1 expression and smoking (*SI Appendix*, Fig. S9 *B* and *C* and Table S4, $P = 0.028$), with higher hISM1 expression observed in current smokers than ex-smokers (*SI Appendix*, Fig. S9*D*). These findings are consistent with ISM1 being up-regulated specifically in mouse AMs upon CS exposure (*SI Appendix*, Fig. S9*E*), while ISM1 staining in other immune cells such as polymorphonuclear leukocytes and lymphocytes remained undetectable (*SI Appendix*, Fig. S9*F*).

Altogether, our results indicate that physiological ISM1 is required for maintaining lung homeostasis by controlling AM number and shaping AM function via csGRP78-mediated apoptosis of csGRP78^{high} AMs. ISM1 deficiency leads to the accumulation of csGRP78^{high}MMP-12^{+} proinflammatory AMs, low-grade pulmonary inflammation, and emphysema in mice under ambient air (Fig. 5). Correspondingly, intratracheal instillation of rISM1 reduced csGRP78^{high} AMs and blocked CS-induced emphysema in mice. We also anticipate that, similar to mice, pulmonary instillation of rISM1 would reduce csGRP78^{high} AM numbers and attenuate tissue damage in the human COPD lung. As GRP78 is a stress-induced protein and csGRP78 is selectively present on stress-activated proinflammatory AMs, rISM1 has the potential to be developed into an AM-directed therapeutic for COPD, targeting csGRP78 to curb lung inflammation.

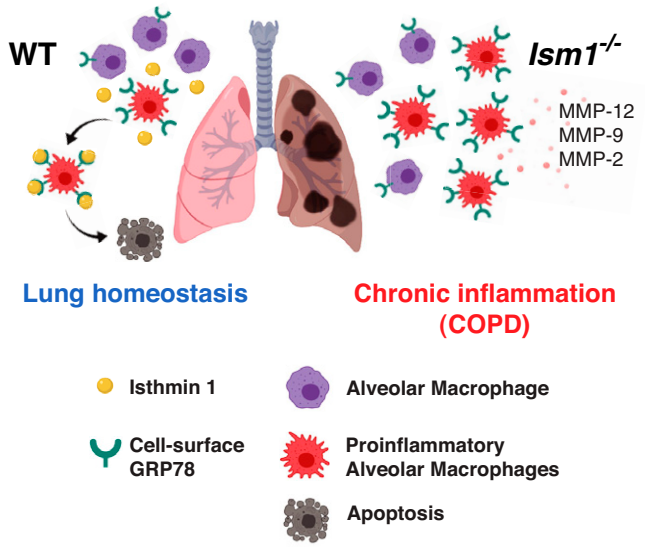

Fig. 5. Proposed mechanism of action for ISM1 in regulating AM apoptosis and lung homeostasis. (*Left*) Autocrine/paracrine ISM1 specifically targets and removes proinflammatory csGRP78^{high} AMs via apoptosis to maintain lung homeostasis. (*Right*) Absence of ISM1 in *Ism1*$^{-/-}$ mice results in diminished apoptosis and accumulation of proinflammatory csGRP78^{high} AMs, leading to proteinases overproduction, emphysema, and lung function decline.

Discussion

Inflammation regulation and homeostasis maintenance are of paramount importance for the lung due to its constant exposure to the external environment. However, how the lung maintains homeostasis remains poorly understood. In this work, we show that the secreted ISM1 is a lung resident anti-inflammatory protein that is critical for maintaining lung homeostasis. ISM1 suppresses lung inflammation by specifically targeting csGRP78^{high} AMs for apoptosis. Pulmonary delivered rISM1 effectively blocks CS-induced emphysema and preserves lung function in mice. These findings not only add insights to the molecular mechanism of COPD pathophysiology but also provide a path for the development of AM-targeted COPD therapeutics.

Numerous studies have demonstrated that AMs are the main orchestrators for COPD, with its number significantly increased as well as function impaired, contributing to chronic lung inflammation even after smoking cessation in COPD patients (24, 38, 39). Hence, AMs are important targets for anti-inflammatory COPD therapeutics. In this work, we show that an increase in csGRP78^{high} AMs in *Ism1*$^{-/-}$ mice because of insufficient ISM1–csGRP78-mediated apoptosis leads to chronic lung inflammation and emphysema. This phenotype is consistent with the increased AM number in COPD patients and previously reported AM apoptosis resistance in COPD (39, 40). In line with this, intratracheally delivered rISM1 induced AM apoptosis and effectively depleted AM accumulation, suppressed emphysema development, and blocked lung function decline in CS-induced COPD mice (Fig. 3). We show that csGRP78^{high} AMs are predominantly MMP-12^{+} and therefore proinflammatory. By selectively inducing csGRP78^{high} AM apoptosis, rISM1 directly impedes proteolytic damage by AM-secreted proteinases such as MMP-12, MMP-9, and MMP-driven TNF-α activation, which is estimated to account for up to 70% of CS-induced lung damage (41). These results concur with a previous report that induced AM apoptosis by intratracheal-delivered alendronate and ameliorated CS-induced emphysema in mice (6). Similarly, the intratracheal instillation of clodronate, another macrophage depletion agent, also reduced AM numbers, suppressed emphysema, and restored lung function (Fig. 3 *A*–*E*) in agreement with other studies (42, 43). Our work here, together with previous studies, demonstrates the beneficial effects of AM depletion in suppressing emphysema in rodent models (6, 42–45).

In a healthy lung, AM numbers are tightly controlled at 0.3 to 1 AM per alveolus in mice, but its regulatory mechanisms remain unknown. Here, we reveal that AMs in a healthy lung express heterogeneous levels of csGRP78, the high-affinity receptor of ISM1 (Fig. 2*J*). As GRP78 is a stress response protein and csGRP78^{high} AMs are predominantly MMP-12^{+}, these csGRP78^{high} AMs are proinflammatory (*SI Appendix*, Fig. S7 *C* and *G*). Consistent with the lung being ISM1's highest expression organ in mice, the loss of ISM1 leads to spontaneous emphysema under ambient air accompanied with excessive csGRP78^{high} AM accumulation. Together with our previous reports that ISM1 specifically targets csGRP78^{high} cells for apoptosis (19, 36), our findings here support a model whereby ISM1 selectively eliminates csGRP78^{high} AMs through apoptosis, while csGRP78$^{low/-}$ AMs are left intact, thus controlling both AM number and integrity to protect lung homeostasis (Fig. 5). These findings underscore the importance of AM population control for lung homeostasis. Even in the absence of environmental assault, deficient AM apoptosis and excessive csGRP78^{high} AM accumulation were sufficient for emphysema development in *Ism1*$^{-/-}$ mice. Nevertheless, future studies to investigate cell-specific deletions of 1) ISM1 and 2) GRP78 are required to truly deduce the effect of ISM1 and GRP78 in AM biology and lung function. Notably, ISM1 is also expressed in bronchial epithelium in mice, and hence, paracrine ISM1–csGRP78 interaction may also play an important role for ISM1 function in lung. In addition, GRP78 is an essential ER chaperon protein for cell survival, and heterozygous deletion or knockdown approaches may be required in order to study its role in AMs and lungs.

csGRP78^{high} AMs are also significantly increased in CS-induced COPD mouse lungs and human COPD patients, and intratracheally instilled rISM1 effectively depleted AMs and rescued emphysema in both *Ism1*$^{-/-}$ mice and CS-induced COPD mice. These findings underscore the pivotal role AM plays in COPD pathogenesis, highlighting the potential of targeting the proinflammatory AM for COPD therapeutic development. These results also support the notion that rISM1 has the potential to be developed into an AM-targeted therapeutic for COPD while csGRP78 could be a useful target for COPD drug development. There has been no successful development of disease-modifying therapeutics for COPD in the past decades. Major challenges exist for COPD drug development because of disease heterogeneity and differences between human COPD and animal models (46, 47). In this case, rISM1 has the advantage of specifically targeting csGRP78 on GRP78^{high} AMs without damaging the innately immunosuppressive GRP78$^{low/-}$ AMs and interstitial macrophages (48). This study demonstrates a common characteristic between CS-induced mouse COPD and human COPD lungs in harboring more csGRP78^{high} AMs (Figs. 3*J* and 4*G*), making this subset of AMs the prime targets for rISM1-mediated apoptosis. Apoptotic AMs could subsequently be cleared via efferocytosis by untargeted or apoptosis-resistant csGRP78$^{low/-}$ AMs. We envision that rISM1 may also suppress AM-mediated inflammation in COPD patients and block disease progression, although a concrete conclusion can only be obtained through clinical trials.

It is noted that endogenous ISM1 may not be sufficient to overcome inflammation in the COPD lung, despite the positive correlation between ISM1 expression and AM apoptosis. This is a common phenomenon in many disease situations such as in a viral infection in which a heightened production of immune

antiviral factors may still not be enough to overcome the viral infection. Accordingly, exogenously supplied rISM1 provided the additional help to further increase AM apoptosis, resulting in effective reduction of lung inflammation and blockage of tissue damage in CS-induced COPD mice.

On the other hand, AMs in COPD are also known to have impaired phagocytosis (engulfing pathogens) and efferocytosis (engulfing apoptotic cells), at least when they are analyzed in cell culture conditions in vitro (49, 50). Whether or not driving AMs toward more apoptosis is beneficial for COPD patients when efferocytosis is impaired will require further investigation through clinical trials. In contrast, *Ism1*$^{-/-}$ AMs harbor similar efferocytosis activity in vitro as WT AMs (*SI Appendix*, Fig. S4*C*). Nevertheless, our study here concurs with multiple previous reports in mouse and rat models that point toward a beneficial effect for COPD when AM apoptosis is enhanced, a result of reduced proteinases and proinflammatory factors in COPD (6, 39, 40, 43–45).

Although previous genome-wide association studies have not associated the *Ism1* locus with COPD, results from this study suggest that it could be meaningful to investigate ISM1 expression in a larger population of COPD patients to uncover any potential genetic or epigenetic influences on *Ism1* and its regulatory genes. Additional studies are also required to determine the exact link between ISM1 expression level and COPD disease severity or phenotype.

It is known that local macrophage apoptosis and clearance contribute to inflammation resolution in atherosclerosis, experimental peritonitis, and infection-associated acute pulmonary inflammation (51–54). Our work here reveals the role of autocrine/paracrine ISM1–csGRP78 signaling in inducing csGRP78^{high} AM apoptosis and maintaining lung homeostasis. ISM1's role in regulating AM apoptosis for lung homeostasis is likely unique to mammals. Previous *Ism1* knockdown studies in lower vertebrates showed phenotypes such as craniofacial defects in *Xenopus* (55) and angiogenesis and hematopoiesis defects in zebrafish (18, 56). The highly divergent and intrinsically disordered N-terminal region of ISM1 (the first 200 residues) may contribute to the diverse biological functions in different vertebrate species (57). On the other hand, high sequence conservation and identity between mouse and human in the thrombospondin type 1 repeat domain (98% identical) and the adhesion-associated domain in Mucin 4 and other proteins domain (99% identical) suggests that ISM1 likely possesses important conserved functions between mouse and human (58).

Although αvβ5 integrin, the low-affinity receptor of ISM1, has also been reported to be present on lung endothelial and airway epithelial cells (59), no αvβ5 integrin expression was detected in AMs nor did we observe any obvious targeting of αvβ5^{+} cells when rISM1 was delivered intratracheally (*SI Appendix*, Fig. S7 *B* and *H*). Consistently, no aggravated emphysema due to undesired apoptosis of structural cells was observed. Instead, rISM1 treatment relieved emphysema and helped to preserve lung function in *Ism1*$^{-/-}$ mice.

One limitation of our study is the delivery of rISM1 via intratracheal instillation to CS-induced COPD mice. Aerosol inhalation would be more relevant for therapeutic delivery for human COPD. Whether rISM1 is suitable for aerosol inhalation remains to be determined. Nevertheless, the relatively large size of rISM1 (~50 kDa) suggests that it would not be rapidly cleared from the lung and absorbed into the bloodstream (60, 61). Significant advances in protein therapeutics for topical lung delivery via nebulization have emerged in various clinical trials. For example, several phase II/III clinical trials of alpha-1 antitrypsin (52 kDa) as an inhaled therapeutic have been conducted for alpha-1 antitrypsin deficiency and cystic fibrosis (62). It is likely that ISM1 could also be suitable for pulmonary delivery via nebulization because of its comparable size to alpha-1 antitrypsin. Although rISM1 inhibited emphysema progression in an 8-wk CS-induced COPD mouse model, the extent of lung function decline in this model is only equivalent to mild COPD patients. It remains to be determined if rISM1 treatments would still be protective when emphysema is more pronounced since COPD mainly affects the older population, and patients are often diagnosed late in advanced disease stages. It is noted that the currently available mouse COPD models can only represent early and mild COPD stages.

Although most of the data in this study are from *Ism1*$^{-/-}$ in the FVB/NTac background, *Ism1*$^{-/-}$ mice in the C57BL/6J background also present spontaneous emphysema, albeit milder with lower emphysema scores (*SI Appendix*, Fig. S1). Correspondingly, the overall AM increase is less pronounced in C57BL/6J mice, yet the proportion of csGRP78^{high} AMs are also similarly expanded (*SI Appendix*, Fig. S6*D*). Importantly, *Ism1*$^{-/-}$ AMs from both mouse strains present increased morphological heterogeneity with more cells of larger sizes and the presence of multinucleated giant cells, features absent in WT mice (Fig. 2 *A* and *B* and *SI Appendix*, Fig. S4*A*). These similarities underscore the protective role ISM1 plays in lung homeostasis. In addition, CS is known to induce varied immune responses between different mouse strains, with BALB/c mice displaying greater susceptibility than C57BL/6 mice via increased AMs and robust time-dependent MMP-12 upregulation (63). Our findings here that the pulmonary delivery of rISM1 effectively impeded CS-induced emphysema in BALB/c mice and that CS induced a heightened immune response in *Ism1*$^{-/-}$ C57BL6/J mice also highlight the protective role of ISM1 in mouse lung.

We also wish to point out that although no gross histological abnormalities were observed in other major organs in *Ism1*$^{-/-}$ mice, it is not clear whether subtle changes exist nor changes that occur at molecular and cellular levels. It is also not known if the other organs would present abnormalities under pathological or stressful conditions.

In summary, our findings here reveal the importance of AM apoptosis regulation in lung homeostasis and the critical role ISM1–csGRP78 signaling plays in controlling AM population and function. We identified *Ism1* as a gene linked to COPD pathogenesis in mice and demonstrate that rISM1 attenuates emphysema, suppresses inflammation, and preserves lung function in CS-induced COPD mice by specifically targeting csGRP78 on stress-activated csGRP78^{high} AMs. We propose that csGRP78 is a potentially useful target for developing COPD therapeutics and that rISM1 could be a prospective biologic drug for COPD. Our findings also have implications for other respiratory disorders driven or contributed by activated and proinflammatory AMs including lung ischemia–reperfusion injury (64), acute lung injury (65), lung fibrosis (66), and asthma (67). csGRP78 has been extensively studied as an anticancer drug target (68–70), and we have previously reported that rISM1 suppressed xenograft cancer growth in mice when delivered intravenously (19). We speculate that pathological overexpression of csGRP78 in noncancerous diseases could also provide therapeutic opportunities for rISM1 to modulate inflammation and curtail diseases.

Materials and Methods

Reagents, mice, mouse lung histology and imaging, lung immune cell quantifications, apoptosis determination, cell culture, gelatin zymography, efferocytosis assay, ISM1 and GRP78 antibody validation, human lung tissue, and statistical analysis can be found in *SI Appendix, SI Materials and Methods*.

Study Design. The primary objective of this study was to determine the physiological function of mammalian *Ism1* using an in-house–generated CRISPR/Cas9-mediated knockout of *Ism1* in two genetic backgrounds (FVB/NTac and

C57BL/6J mice). Sample sizes for all experiments were kept at a minimum of three animals per group for statistical analyses, and *n* numbers are presented on the respective figures and legends. Age- and sex-matched mice were randomly allocated into the experimental groups, and no outliers were excluded from the animal studies. rISM1 rescue experiments for *Ism1*$^{-/-}$ mice were repeated twice and separately analyzed for lung function parameters and histology. The rISM1 treatment of 2-wk and 8-wk CS-induced COPD mice experiments were carried out once with lung function parameters measured and left lung lobes fixed for histology analysis and right lung lobes homogenized for biochemical analysis where relevant. Immune cell quantifications of all mouse experiments were carried out in a blind fashion. Deidentified human lung samples were used for immune cell quantifications, staining, and grading for hISM1 expression. No data were excluded in the human cohort study.

Pulmonary Function Test. Spirometry was performed on FVB/NTac WT and *Ism1*$^{-/-}$ mice as well as experimental COPD WT BALB/cAnNTac mice previously described (37). Briefly, mice were anesthetized with a ketamine-medetomidine mixture (75 mg/kg and 1 mg/kg, respectively), and tracheotomy was performed. The mice were intubated with a cannula and placed in a whole-body plethysmograph connected to the Buxco Forced Maneuver System (Buxco Research Systems). Pulmonary function test parameters were recorded using the FinePointe software (Buxco Research Systems).

Emphysema Rescue in FVB/NTac *Ism1*$^{-/-}$ Mice. Female FVB/NTac *Ism1*$^{-/-}$ 4-wk-old mice were intratracheally given 50 μL phosphate-buffered saline (PBS), 1 μg or 5 μg rISM1 in 50 μL PBS, or 350 μg liposome-encapsulated clodronate in 50 μL PBS twice a week for 4 wk. The pulmonary function test was recorded 24 h after the last day of treatment, and lungs were fixed for histology analyses.

CS-Induced COPD Mouse Model. Female BALB/cAnNTac, FVB/NTac, or C57BL/6J 8-wk-old mice were subjected to 2-wk and/or 8-wk CS exposure as previously described (37). Briefly, mice were whole-body exposed to room air or 4% CS mixed with room air from a total of nine 3R4F reference cigarettes (University of Kentucky, Lexington) daily at a frequency of three 3R4F reference cigarettes every 2 h. This was carried out for 5 consecutive days each week. The pulmonary function test was recorded 24 h after the last day of CS exposure, and lungs were fixed for histology analyses.

Data Availability. All data are included in the manuscript and/or *SI Appendix*. Materials are available on request from the authors.

ACKNOWLEDGMENTS. We thank Drs. John Abisheganaden and Albert Yick Hou Lim from the Department of Respiratory and Critical Care Medicine, Tan Tock Seng Hospital; Drs. Sanjay Chotirmall and Tiew Pei Yee from Lee Kong Chian School of Medicine, Nangyang Technological University; Prof. De Yun Wang, Department of Otolaryngology, Yong Loo Lin School of Medicine, National University of Singapore; and Prof. Wenguang Yin from Guangzhou Medical University, National Key Laboratory for Respiratory Diseases, China, for fruitful discussions. We also thank the Lung Tissue Research Consortium, National Heart, Lung and Blood Institute, NIH for providing the human lung tissue samples. This work was supported in part by Singapore Ministry of Education Grants MOE2017-T2-2-122 and R-154-000-516-112 awarded to R.G. and National Research Foundation Grant R-184-000-269-592 awarded to W.S.F.W. T.Y.W.L., N.N., M.S., S.V., and T.Q. were/are supported by PhD scholarships from the National University of Singapore. S.X. is supported by a PhD scholarship under grant MOE2017-T2-2-122 awarded to R.G. H.Y.P. was supported by the President Graduate Fellowship from the National University of Singapore.

1. A. S. Gershon, L. Warner, P. Cascagnette, J. C. Victor, T. To, Lifetime risk of developing chronic obstructive pulmonary disease: A longitudinal population study. *Lancet* **378**, 991–996 (2011).
2. GBD 2015 Mortality and Causes of Death Collaborators, Global, regional, and national life expectancy, all-cause mortality, and cause-specific mortality for 249 causes of death, 1980-2015: A systematic analysis for the Global Burden of Disease Study 2015. *Lancet* **388**, 1459–1544 (2016).
3. D. Singh *et al.*, Global strategy for the diagnosis, management, and prevention of chronic obstructive lung disease: The GOLD science committee report 2019. *Eur. Respir. J.* **53**, 1900164 (2019).
4. C. F. Vogelmeier *et al.*, Global strategy for the diagnosis, management, and prevention of chronic obstructive lung disease 2017 report: GOLD executive summary. *Eur. Respir. J.* **49**, 1700214 (2017).
5. R. Finkelstein, R. S. Fraser, H. Ghezzo, M. G. Cosio, Alveolar inflammation and its relation to emphysema in smokers. *Am. J. Respir. Crit. Care Med.* **152**, 1666–1672 (1995).
6. M. Ueno *et al.*, Alendronate inhalation ameliorates elastase-induced pulmonary emphysema in mice by induction of apoptosis of alveolar macrophages. *Nat. Commun.* **6**, 6332 (2015).
7. R. D. Hautamaki, D. K. Kobayashi, R. M. Senior, S. D. Shapiro, Requirement for macrophage elastase for cigarette smoke-induced emphysema in mice. *Science* **277**, 2002–2004 (1997).
8. T. Hussell, T. J. Bell, Alveolar macrophages: Plasticity in a tissue-specific context. *Nat. Rev. Immunol.* **14**, 81–93 (2014).
9. A. S. Neupane *et al.*, Patrolling alveolar macrophages conceal bacteria from the immune system to maintain homeostasis. *Cell* **183**, 110–125.e11 (2020).
10. A. Roquilly *et al.*, Alveolar macrophages are epigenetically altered after inflammation, leading to long-term lung immunoparalysis. *Nat. Immunol.* **21**, 636–648 (2020).
11. J. Bhattacharya, K. Westphalen, Macrophage-epithelial interactions in pulmonary alveoli. *Semin. Immunopathol.* **38**, 461–469 (2016).
12. K. Westphalen *et al.*, Sessile alveolar macrophages communicate with alveolar epithelium to modulate immunity. *Nature* **506**, 503–506 (2014).
13. M. Blickensdorf, S. Timme, M. T. Figge, Comparative assessment of aspergillosis by virtual infection modeling in murine and human lung. *Front. Immunol.* **10**, 142 (2019).
14. W. A. Wallace, M. Gillooly, D. Lamb, Age related increase in the intra-alveolar macrophage population of non-smokers. *Thorax* **48**, 668–669 (1993).
15. W. A. Wallace, M. Gillooly, D. Lamb, Intra-alveolar macrophage numbers in current smokers and non-smokers: A morphometric study of tissue sections. *Thorax* **47**, 437–440 (1992).
16. A. C. McQuattie-Pimentel *et al.*, The lung microenvironment shapes a dysfunctional response of alveolar macrophages in aging. *J. Clin. Invest.* **131**, e140299 (2021).
17. P. J. Barnes, Alveolar macrophages as orchestrators of COPD. *COPD* **1**, 59–70 (2004).
18. W. Xiang *et al.*, Isthmin is a novel secreted angiogenesis inhibitor that inhibits tumour growth in mice. *J. Cell. Mol. Med.* **15**, 359–374 (2011).
19. M. Chen *et al.*, Isthmin targets cell-surface GRP78 and triggers apoptosis via induction of mitochondrial dysfunction. *Cell Death Differ.* **21**, 797–810 (2014).
20. L. Osório, X. Wu, Z. Zhou, Distinct spatiotemporal expression of ISM1 during mouse and chick development. *Cell Cycle* **13**, 1571–1582 (2014).
21. S. Venugopal *et al.*, Isthmin is a novel vascular permeability inducer that functions through cell-surface GRP78-mediated Src activation. *Cardiovasc. Res.* **107**, 131–142 (2015).
22. Y. Zhang *et al.*, Isthmin exerts pro-survival and death-promoting effect on endothelial cells through alphavbeta5 integrin depending on its physical state. *Cell Death Dis.* **2**, e153 (2011).
23. P. Gagnon *et al.*, Pathogenesis of hyperinflation in chronic obstructive pulmonary disease. *Int. J. Chron. Obstruct. Pulmon. Dis.* **9**, 187–201 (2014).
24. P. J. Barnes, Inflammatory mechanisms in patients with chronic obstructive pulmonary disease. *J. Allergy Clin. Immunol.* **138**, 16–27 (2016).
25. J. A. Dewhurst *et al.*, Characterisation of lung macrophage subpopulations in COPD patients and controls. *Sci. Rep.* **7**, 7143 (2017).
26. P. G. Woodruff *et al.*, A distinctive alveolar macrophage activation state induced by cigarette smoking. *Am. J. Respir. Crit. Care Med.* **172**, 1383–1392 (2005).
27. W. I. de Boer *et al.*, Transforming growth factor beta1 and recruitment of macrophages and mast cells in airways in chronic obstructive pulmonary disease. *Am. J. Respir. Crit. Care Med.* **158**, 1951–1957 (1998).
28. A. R. Kranenburg, W. I. de Boer, V. K. Alagappan, P. J. Sterk, H. S. Sharma, Enhanced bronchial expression of vascular endothelial growth factor and receptors (Flk-1 and Flt-1) in patients with chronic obstructive pulmonary disease. *Thorax* **60**, 106–113 (2005).
29. M. Guilliams *et al.*, Alveolar macrophages develop from fetal monocytes that differentiate into long-lived cells in the first week of life via GM-CSF. *J. Exp. Med.* **210**, 1977–1992 (2013).
30. T. Suzuki *et al.*, Increased pulmonary GM-CSF causes alveolar macrophage accumulation. Mechanistic implications for desquamative interstitial pneumonitis. *Am. J. Respir. Cell Mol. Biol.* **62**, 87–94 (2020).
31. S. I. Mund, M. Stampanoni, J. C. Schittny, Developmental alveolarization of the mouse lung. *Dev. Dyn.* **237**, 2108–2116 (2008).
32. A. Pozarska *et al.*, Stereological monitoring of mouse lung alveolarization from the early postnatal period to adulthood. *Am. J. Physiol. Lung Cell. Mol. Physiol.* **312**, L882–L895 (2017).
33. U. K. Misra, M. Gonzalez-Gronow, G. Gawdi, S. V. Pizzo, The role of MTJ-1 in cell surface translocation of GRP78, a receptor for alpha 2-macroglobulin-dependent signaling. *J. Immunol.* **174**, 2092–2097 (2005).
34. M. C. Lu *et al.*, Anti-citrullinated protein antibodies bind surface-expressed citrullinated Grp78 on monocyte/macrophages and stimulate tumor necrosis factor alpha production. *Arthritis Rheum.* **62**, 1213–1223 (2010).
35. J. Li *et al.*, The unfolded protein response regulator GRP78/BiP is required for endoplasmic reticulum integrity and stress-induced autophagy in mammalian cells. *Cell Death Differ.* **15**, 1460–1471 (2008).
36. M. Chen *et al.*, Extracellular anti-angiogenic proteins augment an endosomal protein trafficking pathway to reach mitochondria and execute apoptosis in HUVECs. *Cell Death Differ.* **25**, 1905–1920 (2018).
37. H. Y. Peh *et al.*, Vitamin E isoform γ-tocotrienol protects against emphysema in cigarette smoke-induced COPD. *Free Radic. Biol. Med.* **110**, 332–344 (2017).
38. J. Domagała-Kulawik, M. Maskey-Warzechowska, I. Kraszewska, R. Chazan, The cellular composition and macrophage phenotype in induced sputum in smokers and ex-smokers with COPD. *Chest* **123**, 1054–1059 (2003).

39. J. Kojima *et al.*, Apoptosis inhibitor of macrophage (AIM) expression in alveolar macrophages in COPD. *Respir. Res.* **14**, 30 (2013).
40. K. Tomita *et al.*, Increased p21(CIP1/WAF1) and B cell lymphoma leukemia-x(L) expression and reduced apoptosis in alveolar macrophages from smokers. *Am. J. Respir. Crit. Care Med.* **166**, 724–731 (2002).
41. A. Churg *et al.*, Tumor necrosis factor-alpha drives 70% of cigarette smoke-induced emphysema in the mouse. *Am. J. Respir. Crit. Care Med.* **170**, 492–498 (2004).
42. E. L. Beckett *et al.*, A new short-term mouse model of chronic obstructive pulmonary disease identifies a role for mast cell tryptase in pathogenesis. *J. Allergy Clin. Immunol.* **131**, 752–762 (2013).
43. S. Pérez-Rial *et al.*, Role of recently migrated monocytes in cigarette smoke-induced lung inflammation in different strain of mice. *PLoS One* **8**, e72975 (2013).
44. D. Lim, W. Kim, C. Lee, H. Bae, J. Kim, Macrophage depletion protects against cigarette smoke-induced inflammatory response in the mouse colon and lung. *Front. Physiol.* **9**, 47 (2018).
45. A. F. Ofulue, M. Ko, Effects of depletion of neutrophils or macrophages on development of cigarette smoke-induced emphysema. *Am. J. Physiol.* **277**, L97–L105 (1999).
46. P. J. Barnes, Corticosteroid resistance in patients with asthma and chronic obstructive pulmonary disease. *J. Allergy Clin. Immunol.* **131**, 636–645 (2013).
47. P. J. Barnes, New anti-inflammatory targets for chronic obstructive pulmonary disease. *Nat. Rev. Drug Discov.* **12**, 543–559 (2013).
48. F. Quesada Calvo *et al.*, Potential therapeutic target discovery by 2D-DIGE proteomic analysis in mouse models of asthma. *J. Proteome Res.* **10**, 4291–4301 (2011).
49. P. S. Hiemstra, Altered macrophage function in chronic obstructive pulmonary disease. *Ann. Am. Thorac. Soc.* **10**, S180–S185 (2013).
50. J. Jubrail, N. Kurian, F. Niedergang, Macrophage phagocytosis cracking the defect code in COPD. *Biomed. J.* **40**, 305–312 (2017).
51. J. D. Aberdein, J. Cole, M. A. Bewley, H. M. Marriott, D. H. Dockrell, Alveolar macrophages in pulmonary host defence the unrecognized role of apoptosis as a mechanism of intracellular bacterial killing. *Clin. Exp. Immunol.* **174**, 193–202 (2013).
52. K. Hamidzadeh, S. M. Christensen, E. Dalby, P. Chandrasekaran, D. M. Mosser, Macrophages and the recovery from acute and chronic inflammation. *Annu. Rev. Physiol.* **79**, 567–592 (2017).
53. S. Arai *et al.*, A role for the apoptosis inhibitory factor AIM/Spalpha/Api6 in atherosclerosis development. *Cell Metab.* **1**, 201–213 (2005).
54. E. L. Gautier, S. Ivanov, P. Lesnik, G. J. Randolph, Local apoptosis mediates clearance of macrophages from resolving inflammation in mice. *Blood* **122**, 2714–2722 (2013).
55. L. A. Lansdon *et al.*, Identification of *Isthmin 1* as a novel clefting and craniofacial patterning gene in humans. *Genetics* **208**, 283–296 (2018).
56. A. Berrun, E. Harris, D. L. Stachura, Isthmin 1 (ism1) is required for normal hematopoiesis in developing zebrafish. *PLoS One* **13**, e0196872 (2018).
57. M. M. Babu, The contribution of intrinsically disordered regions to protein function, cellular complexity, and human disease. *Biochem. Soc. Trans.* **44**, 1185–1200 (2016).
58. T. Joshi, D. Xu, Quantitative assessment of relationship between sequence similarity and function similarity. *BMC Genomics* **8**, 222 (2007).
59. C. M. Teoh, S. S. Tan, T. Tran, Integrins as therapeutic targets for respiratory diseases. *Curr. Mol. Med.* **15**, 714–734 (2015).
60. N. R. Labiris, M. B. Dolovich, Pulmonary drug delivery. Part I: Physiological factors affecting therapeutic effectiveness of aerosolized medications. *Br. J. Clin. Pharmacol.* **56**, 588–599 (2003).
61. J. S. Patton, C. S. Fishburn, J. G. Weers, The lungs as a portal of entry for systemic drug delivery. *Proc. Am. Thorac. Soc.* **1**, 338–344 (2004).
62. E. Bodier-Montagutelli, A. Mayor, L. Vecellio, R. Respaud, N. Heuzé-Vourc'h, Designing inhaled protein therapeutics for topical lung delivery: What are the next steps? *Expert Opin. Drug Deliv.* **15**, 729–736 (2018).
63. A. Morris *et al.*, Comparison of cigarette smoke-induced acute inflammation in multiple strains of mice and the effect of a matrix metalloproteinase inhibitor on these responses. *J. Pharmacol. Exp. Ther.* **327**, 851–862 (2008).
64. B. V. Naidu *et al.*, Early activation of the alveolar macrophage is critical to the development of lung ischemia-reperfusion injury. *J. Thorac. Cardiovasc. Surg.* **126**, 200–207 (2003).
65. J. Dagvadorj *et al.*, Lipopolysaccharide induces alveolar macrophage necrosis via CD14 and the P2X7 receptor leading to interleukin-1α release. *Immunity* **42**, 640–653 (2015).
66. A. V. Misharin *et al.*, Monocyte-derived alveolar macrophages drive lung fibrosis and persist in the lung over the life span. *J. Exp. Med.* **214**, 2387–2404 (2017).
67. T. Nabe *et al.*, Antigen-specific airway IL-33 production depends on FcγR-mediated incorporation of the antigen by alveolar macrophages in sensitized mice. *Immunology* **155**, 99–111 (2018).
68. M. Sato, V. J. Yao, W. Arap, R. Pasqualini, GRP78 signaling hub a receptor for targeted tumor therapy. *Adv. Genet.* **69**, 97–114 (2010).
69. A. S. Lee, GRP78 induction in cancer: Therapeutic and prognostic implications. *Cancer Res.* **67**, 3496–3499 (2007).
70. R. Ge, C. Kao, Cell surface GRP78 as a death receptor and an anticancer drug target. *Cancers (Basel)* **11**, 1787 (2019).